IEEE ICC® 2025

8–12 June 2025 // Montréal, Québec, Canada

Communications Technologies 4Good

IEEE ComSoc® | IEEE

Temperature-Aware Phase-shift Design of LC-RIS for Secure Communication

Mohamadreza Delbari
Co-authors: Bowu Wang, Nairy Moghadas Gholian, Arash Asadi, and Vahid Jamali

11 June 2025

Table of the content

Introduction

Demands:
Higher data rates and capacity are required in modern communication systems (e.g., 5G, 6G).

To provide higher data rates, expanding available bandwidth through increased frequency is essential.

Demands:

Higher data rates and capacity are required in modern communication systems (e.g., 5G, 6G).

To provide higher data rates, expanding available bandwidth through increased frequency is essential.

Time	**XG**	Aim	Data rate
1979	1G	Voice	2 - 3 kbps
1991	2G	SMS	20 - 40 kbps
1998	3G	Data	0.5 - 3 Mbps
2009	4G	Streaming	20 – 100 Mbps
2019	5G	Sensing	100 – 400 Mbps
2030	6G	Intelligence	1 – 10 Gbps

	Varactor	PIN Diode	MEMS Switch	MEMS Mirror	LC
Tuning time	ns	ns	μs	100s of μs	$>$ 10 ms
Tunability	continuous	discrete (1 bit/diode)	discrete	discrete	continuous
Power consumption	medium	medium	low	low	low
Scalability	low (cost per diode)	low (cost per diode)	medium (encapsulation)	medium (cost per area)	high
Frequency range	few GHz	mm-Wave	mm-Wave	THz	$>$ 10 GHz
Cost	high	high	high	high	low

Comparison of technologies used for the realization of RIS [1].

[1] Alejandro Jiménez-Sáez et al. “RISs with LC Technology: A Hardware Design and Communication Perspective”. In: arXiv:2308.03065 (2023).
[2] Guillermo Blanco-Fernández et al. “Lipidic lyotropic LCs: Insights on biomedical applications”. In: Adv. in Colloid and Interface Sci. 313 (2023), p. 102867.

	Varactor	PIN Diode	MEMS Switch	MEMS Mirror	LC
Tuning time	ns	ns	μs	100s of μs	$>$ 10 ms
Tunability	continuous	discrete (1 bit/diode)	discrete	discrete	continuous
Power consumption	medium	medium	low	low	low
Scalability	low (cost per diode)	low (cost per diode)	medium (encapsulation)	medium (cost per area)	high
Frequency range	few GHz	mm-Wave	mm-Wave	THz	$>$ 10 GHz
Cost	high	high	high	high	low

Comparison of technologies used for the realization of RIS [1].

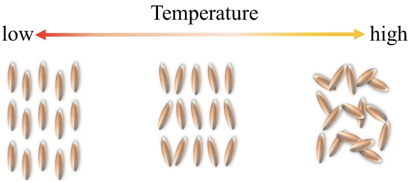

The arrangement of thermotropic LC molecules [2].

[1] Alejandro Jiménez-Sáez et al. "RISs with LC Technology: A Hardware Design and Communication Perspective". In: arXiv:2308.03065 (2023).
[2] Guillermo Blanco-Fernández et al. "Lipidic lyotropic LCs: Insights on biomedical applications". In: Adv. in Colloid and Interface Sci. 313 (2023), p. 102867.

System and LC model

System and LC model

LC model

$$\Delta\omega_{\max} = 2\pi l(\sqrt{\varepsilon_{r,\parallel}} - \sqrt{\varepsilon_{r,\perp}})\frac{f}{c},$$

$$\Delta\omega_{\max}(T) = 2\pi\left(\frac{T_c - T}{T_c - T_r}\right)^{\beta}.$$

T_r: Reference temperature,

T: Current temperature,

T_c: Clearing temperature

β: A physical constant parameter.

[3] Robin Neuder et al. "Architecture for sub-100 ms LC RIS based on defected delay lines". In: Commun. Eng. 3.1 (2024), p. 70.

[4] Henning Tesmer et al. "Temperature characterization of LC dielectric image line phase shifter for mm-Wave applications". In: Crystals 11.1 (2021), p. 63.

System and LC model

LC model

$$\Delta\omega_{\max} = 2\pi l(\sqrt{\varepsilon_{r,\parallel}} - \sqrt{\varepsilon_{r,\perp}})\frac{f}{c},$$

$$\Delta\omega_{\max}(T) = 2\pi\left(\frac{T_c - T}{T_c - T_r}\right)^{\beta}.$$

T_r: Reference temperature,
T: Current temperature,
T_c: Clearing temperature
β: A physical constant parameter.

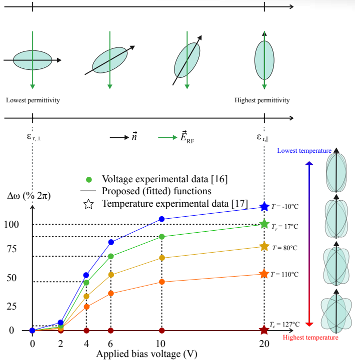

Figure: The relationship between phase shift and applied voltage for an LC at different temperatures is depicted. The experimental data is taken from [3, 4].

[3] Robin Neuder et al. “Architecture for sub-100 ms LC RIS based on defected delay lines”. In: Commun. Eng. 3.1 (2024), p. 70.
[4] Henning Tesmer et al. “Temperature characterization of LC dielectric image line phase shifter for mm-Wave applications”. In: Crystals 11.1 (2021), p. 63.

System and LC model

System model

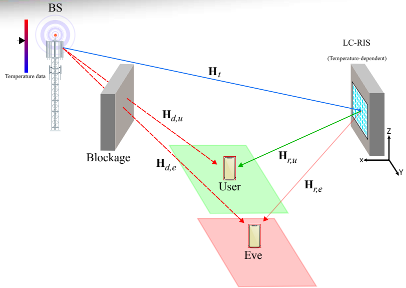

Figure: A schematic of a wireless channel model where an BS serves a legitimate user via an RIS trying to decrease the received signal by an eavesdropper.

System and LC model

System model

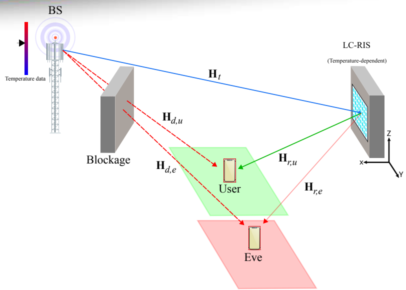

Figure: A schematic of a wireless channel model where an BS serves a legitimate user via an RIS trying to decrease the received signal by an eavesdropper.

$$\mathrm{SR} = [\log(1+\mathrm{SNR}_u) - \log(1+\mathrm{SNR}_e)]^+,$$

$$\mathrm{SNR}_u = \frac{|(\mathbf{h}_u^{\mathrm{eff}})^{\mathsf{H}}\mathbf{q}|^2}{\sigma_n^2},$$

$$\mathrm{SNR}_e = \frac{|(\mathbf{h}_e^{\mathrm{eff}})^{\mathsf{H}}\mathbf{q}|^2}{\sigma_n^2},$$

where $(\mathbf{h}_g^{\mathrm{eff}})^{\mathsf{H}}$, $g = \{u, e\}$ is the end-to-end channel from the BS to the legitimate user and eavesdropper, $\mathbf{q}$ is the BS beamforming signal, and σ_n^2 is the noise power.

System and LC model

System model

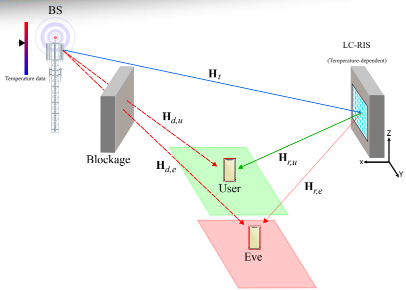

Figure: A schematic of a wireless channel model where an BS serves a legitimate user via an RIS trying to decrease the received signal by an eavesdropper.

$$\mathrm{SR} = [\log(1+\mathrm{SNR}_u) - \log(1+\mathrm{SNR}_e)]^+,$$

$$\mathrm{SNR}_u = \frac{|(\mathbf{h}_u^{\mathrm{eff}})^{\mathsf{H}}\mathbf{q}|^2}{\sigma_n^2},$$

$$\mathrm{SNR}_e = \frac{|(\mathbf{h}_e^{\mathrm{eff}})^{\mathsf{H}}\mathbf{q}|^2}{\sigma_n^2},$$

where $(\mathbf{h}_g^{\mathrm{eff}})^{\mathsf{H}}$, $g = \{u, e\}$ is the end-to-end channel from the BS to the legitimate user and eavesdropper, $\mathbf{q}$ is the BS beamforming signal, and σ_n^2 is the noise power.

Our goal is to maximize the secure rate (SR)

Temperature-aware LC-RIS phase-shift design

Temperature-aware LC-RIS phase-shift design

Problem formulation

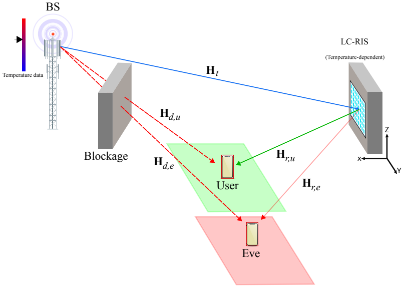

Figure: $\mathcal{P}_u$ and $\mathcal{P}_e$ are the green and red areas, respectively.

Temperature-aware LC-RIS phase-shift design

Problem formulation

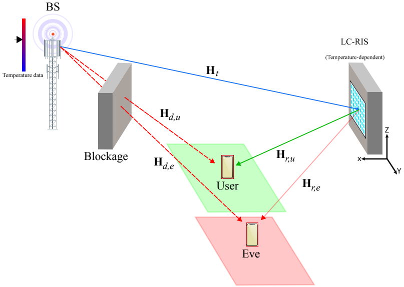

Figure: $\mathcal{P}_u$ and $\mathcal{P}_e$ are the green and red areas, respectively.

$$\text{P1:} \quad \max_{\boldsymbol{\omega},\mathbf{q},\alpha} \alpha$$

$$\text{s.t.} \quad \text{C1: } \mathrm{SR} \geq \alpha, \ \forall \mathbf{p}_u \in \mathcal{P}_u, \ \forall \mathbf{p}_e \in \mathcal{P}_e$$

$$\text{C2: } 0 \leq [\boldsymbol{\omega}]_n < \omega_{\max}, \forall n,$$

$$\text{C3: } \|\mathbf{q}\|_2^2 \leq P_t.$$

α is an auxiliary variable and describes the worst case for the secure rate.

Alternative optimization on BS and RIS

1-Beamformer design:

$$\text{P2:} \quad \max_{\mathbf{q},\alpha} \alpha$$
$$\text{s.t.} \quad \text{C1: } \mathrm{SR} \geq \alpha, \ \forall \mathbf{p}_u \in \mathcal{P}_u, \ \forall \mathbf{p}_e \in \mathcal{P}_e,$$
$$\text{C3: } \|\mathbf{q}\|_2^2 \leq P_t.$$

[5] Mohamadreza Delbari et al. “Temperature-Aware Phase-shift Design of LC-RIS for Secure Communication”. In: arXiv: 2411.12342 (2025).

1-Beamformer design:

$$\text{P2:} \quad \max_{\mathbf{q},\alpha} \alpha$$
$$\text{s.t.} \quad \text{C1: } \mathrm{SR} \geq \alpha, \ \forall \mathbf{p}_u \in \mathcal{P}_u, \ \forall \mathbf{p}_e \in \mathcal{P}_e,$$
$$\text{C3: } \|\mathbf{q}\|_2^2 \leq P_t.$$

Lemma

Assuming a dominant LOS link, fixed RIS phase shifts, and blocked direct channels for both the legitimate user and the eavesdropper, the optimal beamformer for P2 is given by $\mathbf{q} = \sqrt{P_t}\mathbf{a}_{\mathrm{BS}}(\mathbf{p}_{\mathrm{RIS}})$.

Proof.

The proof is provided in [5, Lemma 1]. $\square$

[5] Mohamadreza Delbari et al. "Temperature-Aware Phase-shift Design of LC-RIS for Secure Communication". In: arXiv: 2411.12342 (2025).

2-RIS design:

P3: $$\max_{\boldsymbol{\omega},\alpha} \alpha$$

s.t. C1: $\mathrm{SR} \geq \alpha, \forall \mathbf{p}_u \in \mathcal{P}_u, \forall \mathbf{p}_e \in \mathcal{P}_e$

C2: $0 \leq [\boldsymbol{\omega}]_n < \omega_{\max}, \forall n.$

2-RIS design:

$$\text{P3:} \quad \max_{\boldsymbol{\omega},\alpha} \alpha$$

$$\text{s.t.} \quad \text{C1: } \mathrm{SR} \geq \alpha, \ \forall \mathbf{p}_u \in \mathcal{P}_u, \ \forall \mathbf{p}_e \in \mathcal{P}_e$$

$$\text{C2: } 0 \leq [\boldsymbol{\omega}]_n < \omega_{\max}, \forall n.$$

$$\mathbf{s} \triangleq [\mathrm{e}^{\mathrm{j}[\boldsymbol{\omega}]_1}, \cdots, \mathrm{e}^{\mathrm{j}[\boldsymbol{\omega}]_N}]^{\mathsf{T}},$$

$$\mathbf{S} \triangleq \mathbf{s}\mathbf{s}^{\mathsf{H}},$$

$$\mathbf{A}_g = \frac{\mathrm{diag}(\mathbf{h}_{r,g}^{\mathsf{H}})\mathbf{H}_t\mathbf{q}\mathbf{q}^{\mathsf{H}}\mathbf{H}_t^{\mathsf{H}}\mathrm{diag}(\mathbf{h}_{r,g})}{\sigma_n^2}, \ g = \{u, e\},$$

$$\alpha \triangleq \log(\gamma).$$

2-RIS design:

P3: $\max_{\boldsymbol{\omega},\alpha} \alpha$

s.t. C1: $\mathrm{SR} \geq \alpha,\ \forall \mathbf{p}_u \in \mathcal{P}_u,\ \forall \mathbf{p}_e \in \mathcal{P}_e$

C2: $0 \leq [\boldsymbol{\omega}]_n < \omega_{\max},\ \forall n.$

$$\mathbf{s} \triangleq [\mathrm{e}^{\mathrm{j}[\boldsymbol{\omega}]_1}, \cdots, \mathrm{e}^{\mathrm{j}[\boldsymbol{\omega}]_N}]^{\mathsf{T}},$$

$$\mathbf{S} \triangleq \mathbf{s}\mathbf{s}^{\mathsf{H}},$$

$$\mathbf{A}_g = \frac{\mathrm{diag}(\mathbf{h}_{r,g}^{\mathsf{H}})\mathbf{H}_t\mathbf{q}\mathbf{q}^{\mathsf{H}}\mathbf{H}_t^{\mathsf{H}}\mathrm{diag}(\mathbf{h}_{r,g})}{\sigma_n^2},\ g = \{u, e\},$$

$$\alpha \triangleq \log(\gamma).$$

$$\widehat{\mathrm{C1}} : (1-\gamma) + \mathbf{s}^{\mathsf{H}} \underbrace{(\mathbf{A}_u(\mathbf{p}_u) - \gamma\mathbf{A}_e(\mathbf{p}_e))}_{\mathbf{A}(\gamma)} \mathbf{s} \geq 0,\ \forall \mathbf{p}_u \in \mathcal{P}_u,\ \forall \mathbf{p}_e \in \mathcal{P}_e.$$

$$
\begin{aligned}
\text{P4: } & \max_{\mathbf{S},\gamma} \gamma \\
\text{s.t. } & \widehat{\text{C1}} : \operatorname{tr}(\mathbf{A}(\gamma)\mathbf{S}) \geq \gamma - 1, \forall \mathbf{p}_u \in \mathcal{P}_u, \forall \mathbf{p}_e \in \mathcal{P}_e, \\
& \text{C2: } 0 \leq [\boldsymbol{\omega}]_n < \omega_{\max}, \forall n, \\
& \text{C3: } \mathbf{S} \succeq 0, \text{C4: } \operatorname{rank}(\mathbf{S}) = 1, \text{C5: } \operatorname{diag}(\mathbf{S}) = \mathbf{1}_N.
\end{aligned}
$$

$$
\begin{aligned}
\text{P4: } & \max_{\mathbf{S},\gamma} \ \gamma \\
\text{s.t. } & \widehat{\text{C1}} : \operatorname{tr}(\mathbf{A}(\gamma)\mathbf{S}) \geq \gamma - 1, \forall \mathbf{p}_u \in \mathcal{P}_u, \ \forall \mathbf{p}_e \in \mathcal{P}_e, \\
& \text{C2: } 0 \leq [\boldsymbol{\omega}]_n < \omega_{\max}, \forall n, \\
& \text{C3: } \mathbf{S} \succeq 0, \text{C4: } \operatorname{rank}(\mathbf{S}) = 1, \text{C5: } \operatorname{diag}(\mathbf{S}) = \mathbf{1}_N.
\end{aligned}
$$

$\widehat{\text{C1}}$: Convex,
C2: Non-convex,
C3: Convex
C4: Non-convex,
C5: Convex.

C4: $\mathrm{rank}(\mathbf{S}) = 1$ [6]

$$\text{P5:} \quad \max_{\mathbf{S},\gamma} \gamma - \eta^{(i)} \Big(\|\mathbf{S}\|_* - \|\mathbf{S}^{(i)}\|_2 - \mathrm{tr}\left(\boldsymbol{\lambda}_{\max}(\mathbf{S}^{(i)}) \times \boldsymbol{\lambda}_{\max}^{\mathsf{H}}(\mathbf{S}^{(i)})(\mathbf{S} - \mathbf{S}^{(i)}) \right) \Big)$$

s.t. $\widehat{\widehat{\text{C1}}}$, C2, C3, C5.

[6] Xianghao Yu et al. "Power-Efficient Resource Allocation for Multiuser MISO Systems via IRS". In: Globecom. 2020, pp. 1–6. doi: 10.1109/GLOBECOM42002.2020.9348054.

C4: $\mathrm{rank}(\mathbf{S}) = 1$ [6]

$$\text{P5:} \quad \max_{\mathbf{S},\gamma} \gamma - \eta^{(i)} \Big(\|\mathbf{S}\|_* - \|\mathbf{S}^{(i)}\|_2 - \mathrm{tr}\left(\boldsymbol{\lambda}_{\max}(\mathbf{S}^{(i)}) \times \boldsymbol{\lambda}^{\mathsf{H}}_{\max}(\mathbf{S}^{(i)})(\mathbf{S} - \mathbf{S}^{(i)}) \right) \Big)$$

$$\text{s.t.} \quad \widehat{\widehat{\text{C1}}}, \text{C2}, \text{C3}, \text{C5}.$$

i:	Denoting ith iteration,
$\|\mathbf{S}\|_* = \sum_j \sigma_j$:	Nuclear norm,
$\|\mathbf{S}\|_2 = \max_j \sigma_j$:	Spectral norm,
$\sigma_j, \ \forall j$:	Singular values of $\mathbf{S}$,
$\boldsymbol{\lambda}_{\max}(\mathbf{S})$:	Eigenvector associated with the maximum eigenvalue of matrix $\mathbf{S}$.

[6] Xianghao Yu et al. "Power-Efficient Resource Allocation for Multiuser MISO Systems via IRS". In: Globecom. 2020, pp. 1–6. doi: 10.1109/GLOBECOM42002.2020.9348054.

C2: $0 \leq [\boldsymbol{\omega}]_n < \omega_{\max}, \forall n$ [5]

$$\text{P6:} \quad \max_{\mathbf{S},\gamma} \gamma - \eta^{(i)} \Big(\|\mathbf{S}\|_* - \|\mathbf{S}^{(i)}\|_2 - \mathrm{tr}\left(\boldsymbol{\lambda}_{\max}(\mathbf{S}^{(i)}) \times \boldsymbol{\lambda}^{\mathsf{H}}_{\max}(\mathbf{S}^{(i)})(\mathbf{S} - \mathbf{S}^{(i)})\right)\Big)$$

$$\text{s.t.} \quad \widehat{\widehat{\text{C1}}}, \widehat{\text{C2}}, \text{ C3, C5.}$$

[5] Mohamadreza Delbari et al. "Temperature-Aware Phase-shift Design of LC-RIS for Secure Communication". In: arXiv: 2411.12342 (2025).

C2: $0 \leq [\boldsymbol{\omega}]_n < \omega_{\max}, \forall n$ [5]

P6:
$$\max_{\mathbf{S},\gamma} \gamma - \eta^{(i)} \Big(\|\mathbf{S}\|_* - \|\mathbf{S}^{(i)}\|_2 - \mathrm{tr}\left(\boldsymbol{\lambda}_{\max}(\mathbf{S}^{(i)}) \times \boldsymbol{\lambda}^{\mathsf{H}}_{\max}(\mathbf{S}^{(i)})(\mathbf{S} - \mathbf{S}^{(i)})\right) \Big)$$

s.t. $\widehat{\widehat{\text{C1}}}$, $\widehat{\text{C2}}$, C3, C5.

$$\widehat{\text{C2}} : \mathrm{Re}(\zeta \sum_{i=1}^{N} [\mathbf{S}]_{n,i}) + \tan\left(\frac{\omega_{\max}}{2}\right) \mathrm{Im}(\zeta \sum_{i=1}^{N} [\mathbf{S}]_{n,i}) \leq 1, \forall n,$$

where $\mathrm{Re}(\cdot)$ and $\mathrm{Im}(\cdot)$ denote the real and imaginary parts, respectively.

---

[5] Mohamadreza Delbari et al. “Temperature-Aware Phase-shift Design of LC-RIS for Secure Communication”. In: arXiv: 2411.12342 (2025).

Lemma

Let us assume ω_n is uniformly distributed in interval $[0, \omega_{\max}]$. For sufficiently large N, matrix $\mathbf{S}$ that satisfies the constraints C2-C5, also satisfies:

$$\sum_{i=1}^{N} [\mathbf{S}]_{n,i} = \mathrm{e}^{\mathrm{j}[\boldsymbol{\omega}]_n} \underbrace{\frac{N(1 - \mathrm{e}^{-\mathrm{j}\omega_{\max}})}{\mathrm{j}\omega_{\max}}}_{\zeta^{-1}}, \forall n.$$

Proof.

The proof is provided in [5, Lemma 2] □

[5] Mohamadreza Delbari et al. "Temperature-Aware Phase-shift Design of LC-RIS for Secure Communication". In: arXiv: 2411.12342 (2025).

Lemma

Let us assume ω_n is uniformly distributed in interval $[0, \omega_{\max}]$. For sufficiently large N, matrix $\mathbf{S}$ that satisfies the constraints C2-C5, also satisfies:

$$\sum_{i=1}^{N}[\mathbf{S}]_{n,i} = \mathrm{e}^{\mathrm{j}[\boldsymbol{\omega}]_n} \underbrace{\frac{N(1-\mathrm{e}^{-\mathrm{j}\omega_{\max}})}{\mathrm{j}\omega_{\max}}}_{\zeta^{-1}}, \forall n.$$

Proof.

The proof is provided in [5, Lemma 2] $\square$

Lemma

The constraint $0 \leq [\boldsymbol{\omega}]_n \leq \omega_{\max}$, where $\pi < \omega_{\max} < 2\pi$, is equivalent to $\mathrm{Re}([\mathbf{s}]_n) + \tan\left(\frac{\omega_{\max}}{2}\right)\mathrm{Im}([\mathbf{s}]_n) \leq 1$.

Proof.

The proof is provided in [5, Lemma 3]. $\square$

[5] Mohamadreza Delbari et al. “Temperature-Aware Phase-shift Design of LC-RIS for Secure Communication”. In: arXiv: 2411.12342 (2025).

Performance Comparison

Performance Comparison

Simulation setup

Parameter	**Value**
Frequency	28 GHz
Bandwidth	20 MHz
Transmission Power	40 dBm
BS Antennas (x – z axes)	4×4
RIS Elements (y – z axes)	20×10
Channel Model	Ricean
Path Loss Model	$\rho(\frac{1}{d})^{\sigma}$
Noise Level	-95 dBm
Direct Blockage	- 40 dB
β	0.25
T_c	127°C
T_r	17°C
T	57°C

Performance Comparison

Simulation setup

Parameter	Value
Frequency	28 GHz
Bandwidth	20 MHz
Transmission Power	40 dBm
BS Antennas (x – z axes)	4×4
RIS Elements (y – z axes)	20×10
Channel Model	Ricean
Path Loss Model	$\rho(\frac{1}{d})^{\sigma}$
Noise Level	-95 dBm
Direct Blockage	- 40 dB
β	0.25
T_c	127°C
T_r	17°C
T	57°C

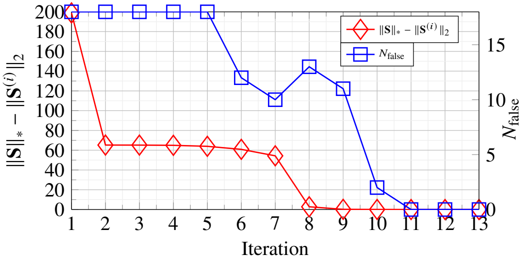

Performance Comparison

Simulation results

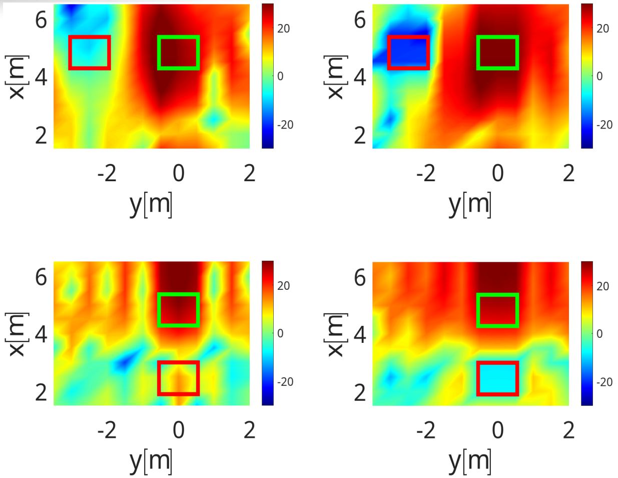

Performance Comparison

Simulation results

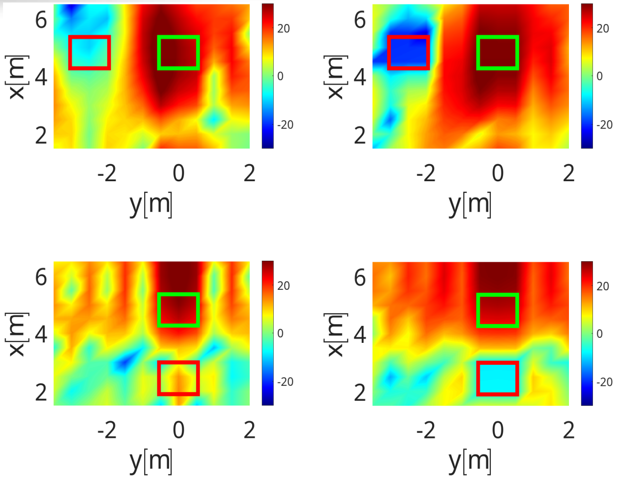

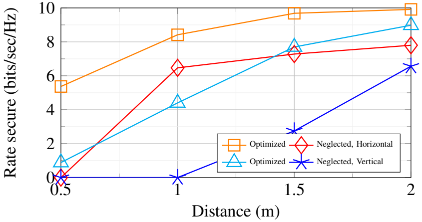

Conclusion and future works

Conclusion and future works

Conclusion

- We need higher frequencies and LCs are one potential way for implementation.
- Despite being good candidates to implement RISs, LC's are sensitive to the temperature.
- We have optimized LC-RIS phase shifts in the secure communication scenario when the temperature is not ideal.

Future works

- Multi-user/eavesdropper case.
- Developing a new algorithm with less complexity.

References I

[1] Alejandro Jiménez-Sáez et al. "RISs with LC Technology: A Hardware Design and Communication Perspective". In: *arXiv:2308.03065* (2023).

[2] Guillermo Blanco-Fernández et al. "Lipidic lyotropic LCs: Insights on biomedical applications". In: *Adv. in Colloid and Interface Science* 313 (2023), p. 102867.

[3] Robin Neuder et al. "Architecture for sub-100 ms LC RIS based on defected delay lines". In: *Commun. Eng.* 3.1 (2024), p. 70.

[4] Henning Tesmer et al. "Temperature characterization of LC dielectric image line phase shifter for mm-Wave applications". In: *Crystals* 11.1 (2021), p. 63.

[5] Mohamadreza Delbari et al. "Temperature-Aware Phase-shift Design of LC-RIS for Secure Communication". In: *arXiv: 2411.12342* (2025).

[6] Xianghao Yu et al. "Power-Efficient Resource Allocation for Multiuser MISO Systems via IRS". In: *Globecom*. 2020, pp. 1–6. DOI: 10.1109/GLOBECOM42002.2020.9348054.

Thank you for your attention

Should you have any questions, please send me via email:

mohamadreza.delbari@tu-darmstadt.de

Link to the paper: